

OPTIMIZING FORCE AND VELOCITY: MANDIBLE MUSCLE FIBRE ATTACHMENTS IN ANTS

JÜRGEN PAUL* AND WULFILA GRONENBERG

*Theodor Boveri Institut der Universität, Lehrstuhl für Verhaltensphysiologie und Soziobiologie, Am Hubland,
D-97074 Würzburg, Germany*

*e-mail: jpaul@biozentrum.uni-wuerzburg.de

Accepted 14 January; published on WWW 3 March 1999

Summary

To be able to perform swift and powerful movements, ant mandible closer muscles are composed of two subpopulations of muscle fibres: fast fibres for rapid actions and slow fibres for forceful biting. All these fibres attach to a sturdy and complex apodeme which conveys force into the mandible base. Fast muscle fibres attach directly to the apodeme. Slow fibres may attach directly or insert at individual thin filament processes of the apodeme which vary in length. Comparisons of different ant species suggest two basic principles underlying the design of mandible muscles. (1) Ants specialized for fast mandible movements generally feature long heads which contain long fast muscle fibres that attach to the apodeme at small angles. Their muscles comprise only a few filament-

attached fibres and they maximize speed of action at the expense of force output. (2) Ants performing particularly forceful mandible movements, such as seed cracking, rely on many short parallel muscle fibres contained within a broad head capsule. Their slower muscles incorporate a large proportion of filament-attached fibres. Two simple models explain how the attachment angles are optimized with respect to force and velocity output and how filament-attached fibres help to generate the largest power output from the available head capsule volume.

Key words: biomechanics, insect, apodeme, ant, feeding, muscle attachment.

Introduction

To many insects, and to ants in particular, mandibles are important tools. Ants use these shovel- or tong-like mouthparts for almost any task, including prey-catching, fighting, digging, leaf-cutting and wood-scraping, as well as for delicate tasks such as grooming, brood care, carrying nestmates or liquids, and communication (Hölldobler and Wilson, 1990). Accordingly, ant mandibles have to perform many different kinds of movements in terms of velocity, power output and precision (Gronenberg et al., 1997). Even though opener–closer muscle co-contraction may occur, the mandible closer muscle is the key to the versatility of mandible movements (Gronenberg et al., 1998b). The mandible closer muscle is much larger than the opener muscle and usually occupies two-thirds of the entire head volume. It is the largest muscle in any ant worker and is always composed of several motor units that may be activated individually, sequentially or synchronously to generate a variety of different types of movement (Just and Gronenberg, 1999).

In almost all ants, the mandible closer muscle is composed of two distinct types of muscle fibre: fibres with long sarcomeres (5–9 µm in length) and fibres with short sarcomeres (2–3 µm). According to their morphological, ultrastructural and biochemical properties, these fibres contract either slowly or relatively rapidly, respectively (Gronenberg and Ehmer,

1995; Gronenberg et al., 1997). In long sarcomeres, more myosin–actin cross-bridges generally act in parallel; therefore, the slow closer muscle fibres generate larger forces. Hence, the closer muscle is composed of two different sets of fibres: powerful slow fibres and less forceful fast ones (Gronenberg et al., 1997). Below, we will refer to the closer muscle fibres with long sarcomeres as slow fibres and to the fibres with short sarcomeres as fast fibres. The fibre distribution and the ratio of fast to slow fibres is species-specific and (besides the overall size of the muscle) determines the maximum contraction velocity and force of the mandibles (Gronenberg et al., 1997).

In addition to the physiological properties of the muscle fibres, the speed and force of a muscle depend strongly on the geometrical arrangement of the muscle fibres and the accessory mechanical structures. The muscle fibre's angle of attachment with respect to the muscle's overall direction of pull is a particularly important determinant of the force that a single fibre contributes. In arthropods, muscle fibres attach to the exoskeleton (e.g. the thorax or head capsule) directly *via* a deeply serrated area of adhesion between the muscle fibre and the cuticle (Neville, 1975; Gronenberg et al., 1997). The opposite end of the muscle fibre connects to a specialized region of the moving body part (e.g. the leg or mandible) referred to as the apodeme, which is the functional analogue

of the vertebrate tendon (Pringle, 1972). In some arthropod muscles, including the ant mandible closer, muscle fibres may connect to thread-like processes of the apodeme rather than attaching to its main body through the entire cross-sectional area (Fig. 1; Janet, 1907a,b; Gronenberg et al., 1997). In principle, all these muscle fibres attach to an individual secondary apodeme branch and we will refer to them as 'filament-attached' fibres to differentiate them from the more common type of 'directly attached' muscle fibres.

The presence of such filament-attached fibres has been described previously in ants (Janet, 1907a,b) and other insects (Snodgrass, 1935), but their functional significance has never been addressed. In the present study, we examine the occurrence and distribution of such fibres among different species of ants and we then discuss their possible functional advantages. We also compare the geometry of mandible closer apodemes across various ant taxa and examine whether different muscle fibre types (fast or slow, directly attached or filament-attached) differ with respect to their attachment angles at the apodeme.

This leads to two simple models which explain why, in general, fast or powerful mandible movements require longer or broader ant heads, respectively, why fast or slow muscle fibres should attach at different angles at the apodeme, and how filament-attached fibres can help to optimize the use of the available head capsule volume and the total power output.

Materials and methods

Measurements were made on the following species of ant: *Myrmecia* sp. (Clark), Myrmeciinae, preserved material only; *Diacamma* sp., *Ectatomma ruidum* (Brown), *Gnamptogenys* sp. (Brown), *Harpegnathos saltator*, *Odontomachus bauri*, *O. chelifer* (Brown), Ponerinae; *Acanthognathus rudis* (Brown and Kempf), *Atta sexdens* (Borgmeier), *Leptothorax sordidulus* (Bernhard), *Pogonomyrmex badius* (Cole), Myrmicinae; *Technomyrmex* sp. (Wheeler), Dolichoderinae; *Camponotus rufipes* (Yasumatsu and Brown), Formicinae. The ants were kept in plaster-of-Paris nests under a 12h:12h L:D photoperiod at 25 °C and 50% relative humidity. They were

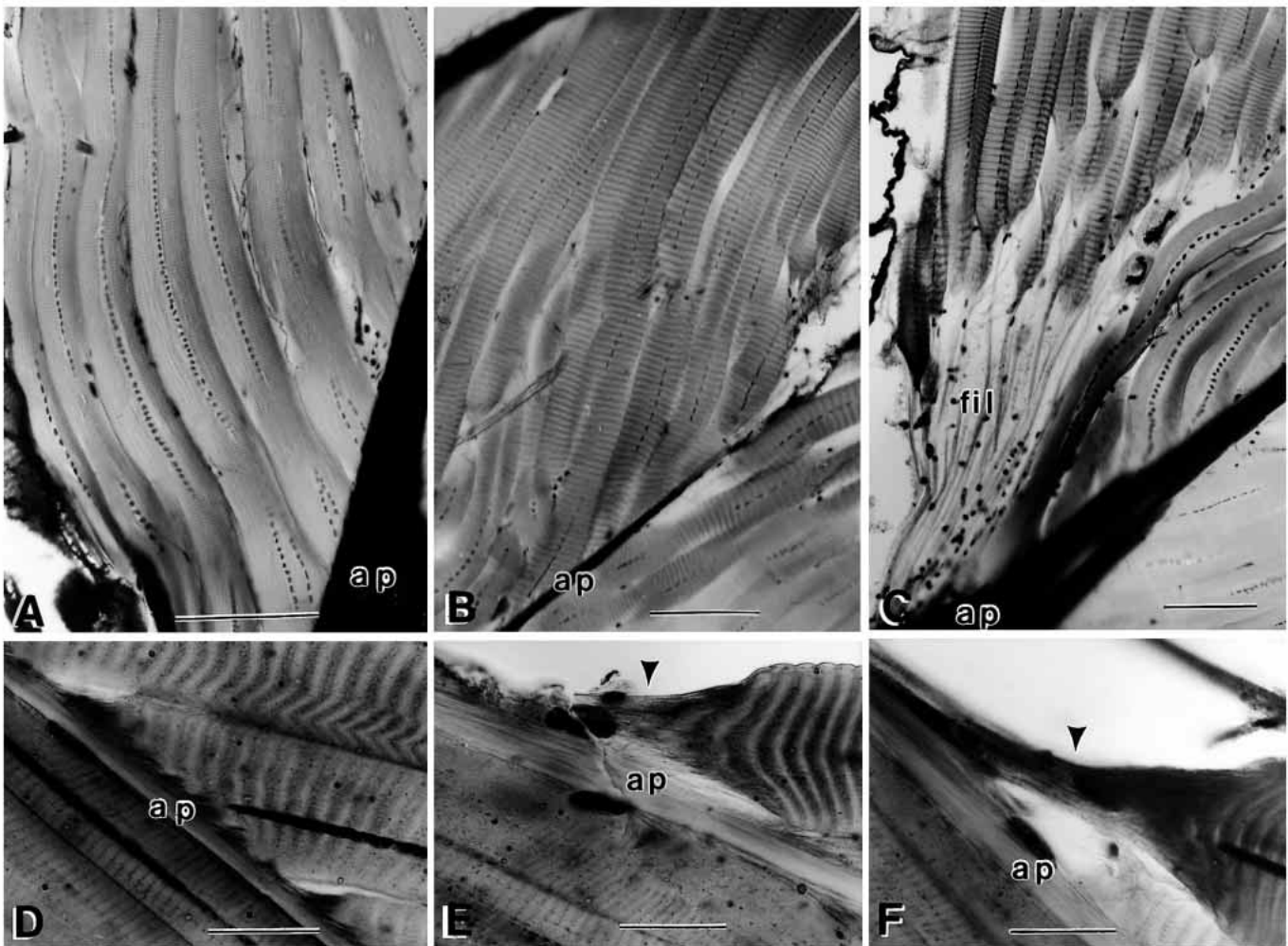


Fig. 1. Photomicrographs of mandible closer muscle fibres. (A) Fast fibres, (B) slow directly attached fibres and (C) filament-attached fibres in *Camponotus rufipes*. (D) Directly attached fibres, (E) fibres with an intermediate attachment and (F) filament-attached fibres in *Myrmecia* sp. ap, apodeme; fil, filament; arrowheads indicate short filaments in E and F. Scale bars, 100 µm (A–C), 20 µm (D–F).

fed chopped cockroaches, crickets or wingless *Drosophila*, and honey-water (30%) or fresh leaves of various kinds (*Atta sexdens*). To examine the morphology of mandible muscles and apodemes within the head, ants were decapitated, and the head capsule was opened under fixative (buffered 4% formaldehyde or 2.5% glutaraldehyde). The heads were then stained either with Methylene Blue or with osmium/ethyl gallate according to Gronenberg (1995) or silver-impregnated (Gronenberg et al., 1997), dehydrated, embedded in Fluka Durcupan and horizontally or vertically sectioned at 10–15 μm . Specimens were drawn from microscopic images using a camera lucida attachment to the microscope (Zeiss Axiophot). The acute angle between the longitudinal axis of the apodeme and the muscle fibre (here referred to as the attachment angle of a muscle fibre) was determined from these drawings. Muscle cross-sectional area was traced from digitized microscopic video images (Gronenberg et al., 1997), and muscle volumes were calculated using the section thickness. We analyzed two or three animals per species with a few exceptions: two minor and three major workers each for *Atta sexdens* and *Camponotus rufipes*, and only a single specimen each for *Pogonomyrmex badius*, *Technomyrmex* sp. and *Gnamptogenys* sp.

Results

The volume of the mandible closer muscle is correlated with the body size of the ant worker, taking up approximately two-thirds of the head volume. This is not the case in most male ants, which have reduced mandibles, and in very small ants. In both these groups, the brain occupies a larger portion of the head than it does in 'normal' workers. Accordingly, the overall volume of the closer muscle varies greatly among species (Table 1): the smallest muscle among the species sampled was found in

Leptothorax sordidulus (total volume 0.01 mm³ per hemisphere) and the largest in a major *Atta sexdens* (4 mm³ per hemisphere). As a result of polymorphism, even within a single colony the size of the closer muscle was found to differ by more than a factor of 30 between soldiers and small workers of *Camponotus rufipes* (Table 1). In *Atta sexdens*, the maximum intra-specific difference will probably be greater than indicated in Table 1 as we did not examine minors, the smallest worker subcaste (Wilson, 1985). The number of closer muscle fibres also depends on the size of the ants. The muscle may be composed of as little as 80 muscle fibres (*Leptothorax sordidulus*) or more than 1000 fibres (*Myrmecia* sp. and *Atta sexdens* major workers). The closer muscle fibres originate from all over the posterior two-thirds of the head capsule and are oriented towards the apodeme in an antero-frontal direction. Before discussing the different fibre types and their distribution within the muscle, we will first describe the mandible closer apodeme in more detail.

Composition of the apodeme

In all species, the mandible closer apodeme follows a basic plan that may be modified to a greater or lesser extent (Fig. 2). A broad, unsclerotized, flexible ligament connects the inner flank of the mandible base to the apodeme base. This main body of the apodeme is a massive sclerotized structure which funnels the forces of all the closer muscle fibres into the mandible. The apodeme base gives rise to apodeme collaterals. Typically, three branches project from the apodeme base posteriorly into the closer muscle: a central principal branch and two accessory branches, a median and a lateral branch. This pattern can be seen best in *Myrmecia* sp., the most primitive ant in our study (Fig. 2), in which the principal branch is the thickest apodeme process. Like the apodeme base, it is often partly sclerotized and it projects in the direction in which the largest forces are to

Table 1. Absolute volumes of mandible closer muscles and their relative compositions with respect to attachment type in different ant species

Species	N	Muscle volume $\times 10^{-6}$ (μm^3)	Directly attached (%)	Filament-attached (%)
<i>Odontomachus chelifer</i>	2		99.3 \pm 0.5	0.7 \pm 0.5
<i>Myrmecia</i> sp.	2	1710 \pm 46	94.6 \pm 1.3	5.4 \pm 0.7
<i>Diacamma</i> sp.	3	355 \pm 3	89.7 \pm 0.9	10.3 \pm 1.0
<i>Harpegnathos saltator</i>	3	1291 \pm 159	83.2 \pm 0.9	16.8 \pm 1.8
<i>Ectatomma ruidum</i>	3	282 \pm 11	65.0 \pm 0.7	35.0 \pm 1.0
<i>Technomyrmex</i> sp.	1		37.8	62.2
<i>Pogonomyrmex badius</i>	1		37.3	62.7
<i>Camponotus rufipes</i> (soldier)	3	954–3244	23.3 \pm 1.8	76.7 \pm 2.6
<i>Gnamptogenys</i> sp.	1		18.4	81.6
<i>Camponotus rufipes</i> (worker)	2	98–157	17.3 \pm 1.1	82.7 \pm 2.2
<i>Atta sexdens</i> (major)	3	1091–3889	10.3 \pm 1.8	89.7 \pm 1.8
<i>Atta sexdens</i> (minor)	2	182–796	8.1 \pm 0.7	91.9 \pm 0.7
<i>Leptothorax sordidulus</i>	3	10.5 \pm 0.2	6.3 \pm 0.2	93.7 \pm 0.4

Values are means \pm S.D.

Measurements were made on one side of the head only.

Size differences between individuals of *C. rufipes* and *A. sexdens* were too large to calculate a meaningful mean value; therefore, a range is given for these species.

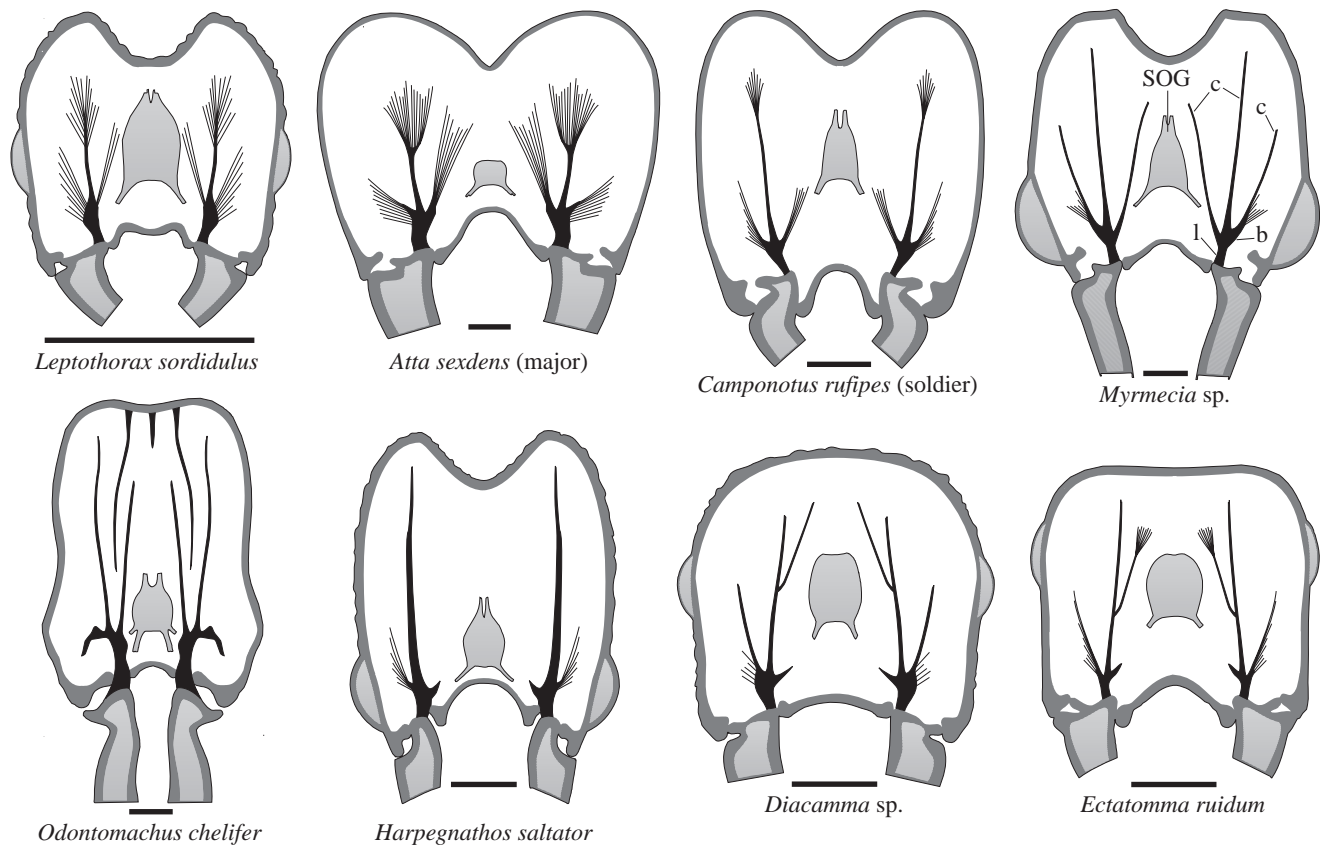


Fig. 2. Schematic dorsal views of heads of different ant species (mid-horizontal plane corresponding to the plane indicated by arrows in Fig. 3F) depicting the organization of the mandible closer apodemes (solid black); b, apodeme base; c, apodeme collateral branches; l, flexible apodeme ligament; SOG, suboesophageal ganglion. Scale bars, 500 μ m.

be expected. The sturdy nature and usual orientation of the principal apodeme branch can be seen clearly in *Harpegnathos saltator* (Fig. 2). This principal branch receives the majority of muscle fibres. In cross section, it is not circular as might be suggested by the dorsal views in Fig. 2. Rather, the principal branch extends in a dorso-ventral direction and is ribbon- or velum-like, depending on the size of the ant and the number of muscle fibres that attach to it. Fig. 3F shows that, in the vertical plane, the principal apodeme branch in *Camponotus rufipes* is slightly S-shaped and tilted with respect to the dorso-ventral axis. The two accessory apodeme branches vary in length between species but are always shorter than the principal one. They are unsclerotized, narrower in the dorso-ventral axis (less velum-like) and connect to fewer muscle fibres.

Among different species, the most variation from this basic apodeme design is in the accessory branches (Fig. 2). In the genera *Diacamma*, *Ectatomma* and *Harpegnathos*, the inner accessory branch is greatly shortened. In the former two genera, the principal branch is slightly bent centrally, compared with other genera, and it carries an additional side branch (Fig. 2). In *Ectatomma ruidum*, muscle fibres attach only to the tip of this additional branch, while in *Diacamma* sp. muscle fibres attach all along its length.

The most significant alteration to the basic design is the introduction of apodeme filaments. Bundles of such filaments,

each of which connects exclusively to a single muscle fibre, may replace the accessory branches entirely, although the basic organization can still be discerned. In the genera *Ectatomma* and *Harpegnathos*, filaments replace the lateral apodeme branch, and in *Atta*, *Camponotus* and *Leptothorax*, both accessory branches are replaced by apodeme filaments (Fig. 2). In the latter three genera, even the principal apodeme branch is shortened and its tip fans out into filaments. The tendency to substitute longer apodeme branches for filaments is most pronounced in *Atta sexdens*, where the filaments are longest and approximately 90% of the muscle fibres are filament-attached (Table 1). Filament length varies across species as well as within individual muscles. Besides *Atta*, other myrmecine genera and the formicine *Camponotus* (Fig. 1) feature long apodeme filaments, while many ponerines have short filaments. In some species, most notably *Myrmecia* sp., all permutations from directly attached to filament-attached fibres exist (Fig. 1D–F). As for filament length, the proportion of filament-attached fibres is smaller in ponerines than in the other subfamilies (Table 1). Likewise, smaller species (*Leptothorax sordidulus*, *Gnamptogenys* sp. and *Technomyrmex* sp.) and smaller individuals (small workers of *Camponotus rufipes*) appear to have relatively more filament-attached muscle fibres (Table 1), while *Myrmecia* sp. and the large ponerines (*Diacamma* sp. and *Harpegnathos saltator*) feature relatively small proportions of these fibres.

The ponerine *Odontomachus chelifer* has the smallest percentage of filament-attached fibres (Table 1), which is probably a derived trait. *Odontomachus chelifer* possesses a highly specialized trap-jaw mechanism which also involves other modifications to the closer apodeme (Fig. 2). Unlike in other ants, the lateral accessory apodeme branch is very strong and sclerotized. Instead of projecting postero-laterally, it forms a hook-like structure that is bent anteriorly and is adapted for the introduction of lateral forces into the mandible. Similarly, the apodeme of *Acanthognathus rudis* features a massive rigid lateral arm allowing slight rotation of the mandible around its long axis in addition to the usual closing movement (Dietz and Brandão, 1993; Gronenberg et al., 1998a). *Odontomachus chelifer* also has three apodemes that originate from the rear of the head (Fig. 2). A large ribbon-like apodeme projects deeply into the head capsule on either side and a shorter one resides medially at the posterior head wall. The large apodemes run between and almost parallel with the two mandible closer apodeme branches. Functionally, these additional apodemes enlarge the surface area of the head capsule substantially to allow the attachment of more closer muscle fibres.

Positions and attachment angles of different fibre types

According to their mode of attachment at the apodeme and to their contraction properties mentioned in the Introduction, muscle fibres can be subdivided into three basic types: fast or slow directly attached fibres and slow filament-attached fibres. No fast fibres attach to the apodeme *via* filaments; the reason for this will be discussed below. Filament-attached fibres are the only fibre type that occurs in the mandible closer muscle of all ants. The three fibre types (fast or slow directly attached and slow filament-attached fibres) are not arbitrarily distributed within the closer muscle but are organized in homogeneous bundles of similar parallel fibres. In general, these fibre groups occupy specific positions, irrespective of the species examined; they are shown for a soldier of *Camponotus rufipes* in Fig. 3A,F. The ratio of the different fibre types varies among species, but is very similar for all workers of a given species even if large size differences exist among them, giving species-specific distribution patterns of fibre types (Fig. 3G). Among the species examined, only for *Camponotus rufipes* does the closer muscle differ between soldiers and small workers. The closer muscles of the latter do not contain any slow directly attached fibres.

If present, fast fibres occur in a similar position within the mandible closer muscle: they originate from the back of the head and project anteriorly over a long distance until they attach at either side of the principal apodeme branch or at the apodeme base proper (fibre groups 1 and 2 in Fig. 3A). The fast fibre bundles are always the longest fibres; they form the centre of the entire closer muscle and are surrounded by fibres of the other two types. The cross sections of the fast fibre bundles are almost circular (Fig. 3F). With the mandibles closed, the attachment angle is $24.8 \pm 8.1^\circ$ (mean \pm S.D.; $N=121$) for the fast fibres of all species examined. Most species have

a similar attachment angle (Table 2). However, some species feature extreme angles of attachment. In the fast predators *Harpegnathos saltator* and *Myrmecia* sp., the angle is very small (approximately 15° ; Table 2). Among ants possessing 'regular' mandibles (as opposed to trap jaws), the largest attachment angles of fast fibres were found in *Atta sexdens* and *Pogonomyrmex badius* (Table 2), which do not perform fast mandible movements (Gronenberg et al., 1997).

The positions of slow directly attached fibres are more variable than those of the other two fibre types. As a consequence of their direct attachment at the apodeme, they are most often found close to the fast fibres. They may be assembled in fibre bundles, as is the case in *Camponotus rufipes* (fibre groups 7, 8 in Fig. 3A,F). Their angle of attachment at the apodeme depends on their position and varies from 20° to 50° with a mean value of $29.6 \pm 8.9^\circ$ ($N=197$) in all the species examined. For these fibres, the largest angles of attachment were found in *Odontomachus chelifer* (46° ; Table 2). In this genus, the mandible closer muscle is composed almost entirely of slow directly attached fibres which are relatively short compared with those of other genera. The same is true for *Acanthognathus rudis*, the other trap-jaw ant examined in the present study (Table 2).

Like the fast fibres, slow filament-attached fibres are also found in particular locations within the mandible closer muscle. In all species, they occupy peripheral positions and thus surround the fast fibre bundles dorsally, ventrally, laterally and (in *Atta sexdens*, *Camponotus rufipes* and *Leptothorax sordidulus*) centrally (fibre groups 3, 4, 9 and 10 in Fig. 3A,F). This organization is illustrated by the dorso-ventral distribution of different fibre types in *Camponotus rufipes* (Fig. 3G). Directly attached fibres are restricted to median head regions which coincide with the principal apodeme branch, while filament-attached fibres are most abundant on the dorsal and

Table 2. Angles of attachment of fast mandible closer muscle fibres at the apodeme in different ant species

Species	N	Angle of attachment (degrees)
Fast directly attached fibres		
<i>Myrmecia</i> sp.	20	14.9 \pm 2.8
<i>Harpegnathos saltator</i>	17	15.8 \pm 3.6
<i>Diacamma</i> sp.	13	21.2 \pm 2.7
<i>Ectatomma ruidum</i>	15	22.7 \pm 3.4
<i>Pachycondyla villosa</i>	7	23.7 \pm 6.2
<i>Camponotus rufipes</i>	22	24.6 \pm 4.2
<i>Atta sexdens</i>	15	36.9 \pm 9.3
<i>Pogonomyrmex badius</i>	12	38.4 \pm 8.2
Slow directly attached fibres		
<i>Acanthognathus rudis</i>	61	40.7 \pm 6.6
<i>Odontomachus chelifer</i>	44	46.1 \pm 9.2

Values are means \pm S.D.; N is the number of fibres examined; the trap-jaw ants *Acanthognathus rudis* and *Odontomachus chelifer* possess only slow fibres (the few specialized fast fibres in these ants serve a different function).

ventral side of the head. In addition, in most myrmicines and formicines, two groups of short filament-attached fibres are found at the distal end of the principal apodeme branch (Fig. 2;

fibre groups 5 and 6 in Fig. 3A). Filament-attached fibres are generally short and feature the largest angles of attachment: up to 75° for lateral fibre groups (group 3 in Fig. 3A) when the

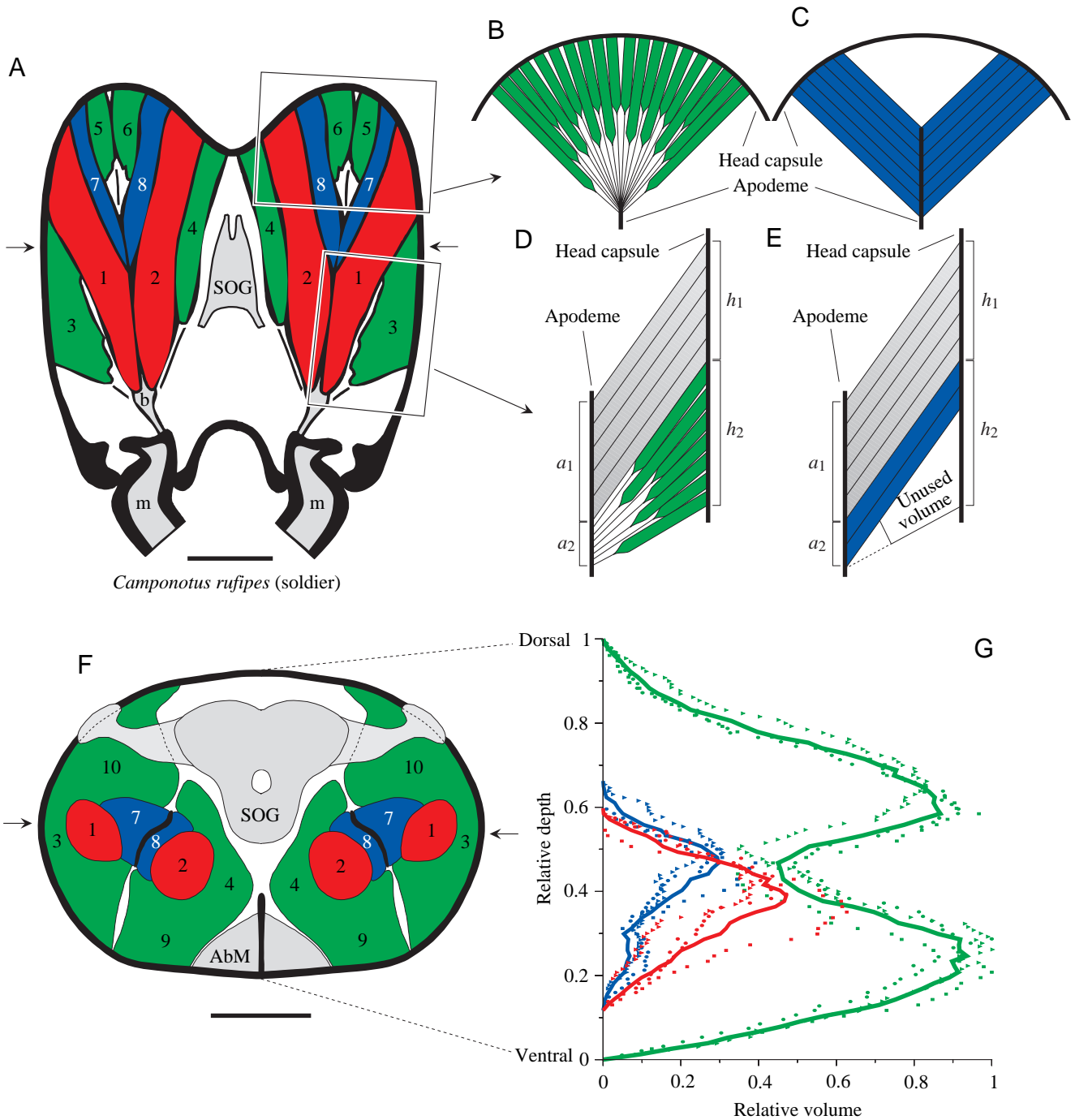


Fig. 3. Organization of mandible closer muscle fibres in the head of *Camponotus rufipes* (soldier). (A) Dorsal view in the plane indicated by arrows in F; (B–E) diagrams illustrating the advantage of filament-attached fibres in the regions marked by rectangles in A (for further details, see text); (F) anterior view in the plane indicated by arrows in A; (G) relative distribution of different closer muscle fibre types calculated from serial section of three specimens: red, fast fibres; blue, slow directly attached fibres; green, slow filament-attached fibres; individual values are represented by symbols; solid lines represent mean values. The x axis shows the relative volume of the respective fibre type in a single section (1 is the highest value found for filament-attached fibres in any section of that animal); the y axis shows the relative dorso-ventral depth (0 is ventral, 1 is dorsal, corresponding to the section in F). Symbols used in D and E: a_1 , a_2 , apodeme surface areas 1 and 2; h_1 , h_2 , corresponding head capsule surface areas 1 and 2. Muscle fibre types in A and F: red, 1, 2, fast; blue, 7, 8, slow directly attached; green, 3–6, 9, 10, filament-attached; AbM, mandible opener muscle; b, apodeme base; m, mandible; SOG, suboesophageal ganglion. Scale bars, 500 μ m.

mandibles are closed (closer muscle contracted; in the open position, no closer muscle fibres of any type feature attachment angles greater than 40°). Some filament-attached fibres are oriented in the direction of pull (groups 5 and 6 in Fig. 3A); for these fibres, the attachment angle may be as small as 0°. Overall, variation in attachment angle is largest in slow filament-attached fibres.

Discussion

Apodeme design: force and velocity require different angles of attachment

The apodeme projects deeply into the closer muscle, and the muscle fibres attach to it at varying angles. Our results suggest that these angles are not arbitrary but are characteristic for a particular fibre type. What determines this angle of attachment and why is it different in different fibre types?

The optimal angle of attachment for any muscle fibre would be 0°, which is parallel to the principal direction of pull. Such a fibre arrangement is shown on the left of Fig. 4C, where all muscle fibres act in that optimal direction. However, this pattern is not found in any arthropod for two reasons. (1) The apodeme is composed of cuticle (Neville, 1975; Snodgrass, 1935) which, even if sclerotized (having cross-linked chitin

filaments), is most stable in the direction parallel to the fibrils (Alexander, 1988; Neville, 1975). A thin sheet-like apodeme, as shown in blue on the left of Fig. 4C, would become bent upon contraction of the muscle rather than transmitting the force into the mandible. To function, a muscle fibre arrangement of this kind would require an extremely thick apodeme, taking up space and representing an additional load which would reduce the advantage given by the muscle fibre's optimal angle of attack. (2) During contraction, such a muscle would swell considerably perpendicular to the direction of contraction because muscle volume remains almost constant while it shortens (Alexander, 1983; Baskin and Paolini, 1966). This, however, is not possible in the restricted space of the inflexible head capsule, which would either prevent the muscle from shortening or crack. In contrast, a muscle of the design shown on the right of Fig. 4C will not swell during contraction (Alexander, 1988).

To understand the design of arthropod muscles, we must first look at the geometrical requirements of single muscle fibres: a muscle will be fast if it consists of particularly long fibres composed of short sarcomeres (many units simultaneously shortening in series; Jahromi and Atwood, 1969; Lang et al., 1977) that attach to the apodeme at small angles; the absolute amount by which the muscle shortens is

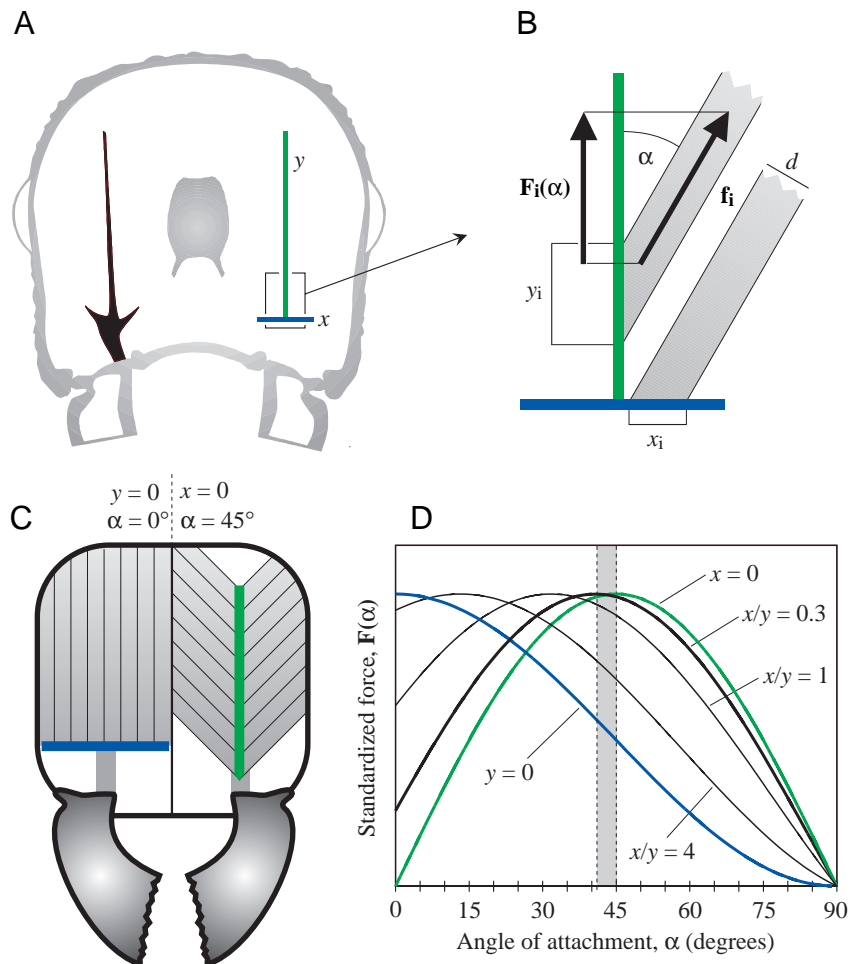


Fig. 4. The effects of apodeme design and fibre angle of attachment on force production. (A) Schematic dorsal view of the mid-horizontal plane of an ant head showing horizontal (blue, x) and vertical (green, y) apodeme components. (B) Muscle fibre forces produced in the apodeme components indicated by the rectangle in A. f_i , force generated by a single fibre; $F_i(\alpha)$, force in the principal direction of pull; α , angle of fibre attachment; d , fibre diameter; x_i , y_i , attachment surface area of a fibre in the x and y direction, respectively. (C) Diagrammatic representation of the head showing attachment angles $\alpha=0^\circ$ and 45° . (D) Force output (normalized to the maximum of the curve for $x=0$) for apodemes with varying x/y composition; the range of x/y ratios found in most ants lies between the green and the thick black lines; the shaded area ($x/y=0-0.3$) shows the corresponding range of optimal angles of attachment for maximal force output. The equation for the graphs in D is derived in the Appendix (equation 6).

thus maximized. An apodeme filament would shorten the contractile part of the muscle fibre and thus remove its fast properties. For this reason, fast fibres are never filament-attached. In contrast, a strong muscle requires many parallel fibres which may be short and are composed of long sarcomeres. In long sarcomeres, the many cross-bridges act in parallel even though, morphologically, they are arranged in rows (Huxley, 1965, 1974; Jahromi and Atwood, 1969; Tregear and Marston, 1979).

The angle of attachment at the apodeme is crucial to the overall force generation of the entire muscle because the apodeme surface area is limited. The significance of the attachment angle can best be explained using a simple model for directly attached muscle fibres (model 1, see Appendix). The total force $F(\alpha)$ of the muscle depends on the individual force of each single fibre f_i , the fibre diameter d , the apodeme composition of horizontal x and longitudinal y components (Fig. 4A,B), and the angle of attachment α , where $F(\alpha) = (f_i/d)(\cos\alpha)[2y(\sin\alpha) + x(\cos\alpha)]$ (see equation 6 from model 1 in the Appendix).

From this equation, it can be shown that the optimal angle of attack for maximum force output depends on the ratio of the x and y components of an apodeme. Fig. 4D shows the standardised force produced by five different apodeme designs; the optimal angle of fibre attachment is that giving maximum force production. If the apodeme has only an x component ($y=0$; blue line in Fig. 4D), the optimal angle is 0° (see above for why this design is not feasible); if the apodeme has only a y component ($x=0$; green line in Fig. 4D; representing species in which there is a principal apodeme branch only and no apodeme base), the optimal attachment angle would be 45° .

For real apodemes, all of which have a small x component ($x/y < 0.3$), the optimum fibre attachment angle is between 41° and 45° for maximum force output (shaded region in Fig. 4D). However, to maximize the shortening velocity, the angle of attachment should approach 0° (see above). Hence, small mean attachment angles indicate fast muscle characteristics because the attachment angle is minimized at the expense of overall force output (at acute angles, fewer fibres can attach directly to the apodeme).

The smallest angles of attachment were found in *Harpegnathos saltator* and *Myrmecia* sp. (Table 2) whose fast fibres deviate by up to 30° from the predicted optimum angle for maximized force (45°). Ants of both genera are fast predators that snap at their prey (Gray, 1971a,b; Gronenberg et al., 1997) and are even able to snatch flying prey from the air (Ali et al., 1992; Tautz et al., 1994; Baroni Urbani et al., 1994). Hence, they depend on the speed of their muscles for their success as hunters. In *Camponotus rufipes*, the fast muscle fibres attach at 25° . These ants are not specialized in terms of mandible function, and the attachment angle represents a compromise between speed and force of action. The herbivorous *Pogonomyrmex badius* and *Atta sexdens* had the largest angles of attachment. The fast fibres in these species attach at almost 40° , close to the predicted force

optimum, indicating that they are specialized for the production of the high forces required to crack seeds (*Pogonomyrmex badius*) or to cut leaves (*Atta sexdens*). In this respect, the mandible closer muscle of *Odontomachus chelifer* also is designed for maximum force production. It is composed of many short parallel fibres which attach at an angle of 46° (Table 2), almost exactly the angle for optimal force output. The apodeme of *Odontomachus chelifer* is almost exclusively composed of the y component, which is possible because of the long internal processes of the head capsule and the elongated head (Fig. 2). A similar design is found in *Acanthognathus rudis*, the other trap-jaw ant in the present study. Hence, like the biochemical and physiological characteristics of muscle fibres, the angle of attachment of muscle fibres allows insights into their function in terms of speed versus force output.

Muscle fibre attachment: why apodeme filaments?

The presence of filament-attached muscle fibres in ants and even some aspects of their development have been known for a long time (Janet, 1905, 1907a,b) and have become textbook knowledge for insects in general (Gullan and Cranston, 1994). However, these muscle fibre attachments have always been treated as 'mere' idiosyncratic features of some insect taxa, and no concepts regarding their functional significance have ever been published.

Ant heads, and elongated ones in particular, contain regions in which the apodeme surface area and the head capsule area are approximately equal (regions a_1 and h_1 in Fig. 3D,E). In these regions, muscle fibres preferentially attach directly to the apodeme because directly attached fibres make the best use of the head capsule volume relative to filament-attached fibres where part of the available space is taken up by filaments and the spaces between them rather than by contractile muscle fibre material.

The apodeme filaments are composed of unsclerotized cuticular material and are therefore flexible and can easily follow movements of the apodeme. This is of particular importance for fibres such as the lateral fibres that attach at large angles (group 3 in Fig. 3A). Such fibres are subjected to larger angular changes when the apodeme moves during mandible closing. This explains why filament-attached fibres are found in this location in all ant species (Fig. 2).

The heads of almost all ants also contain regions where the inner surface of the head capsule provides more area for muscle attachment than does the apodeme. In our model (Fig. 3D,E), this is represented by $a_2 < h_2$. Such an arrangement often is found at the muscle periphery and where the curvature of the head capsule is large (most notably at the posterior end of the head; Fig. 3B,C). Whereas directly attached fibres require attachment surface areas of a similar size at the apodeme and at the head capsule, filament-attached fibres can be found where the ratio of apodeme to head capsule surface area is small because they minimize the apodeme surface area required. They help to fill the head capsule with muscle fibres in regions that would otherwise remain unused because too

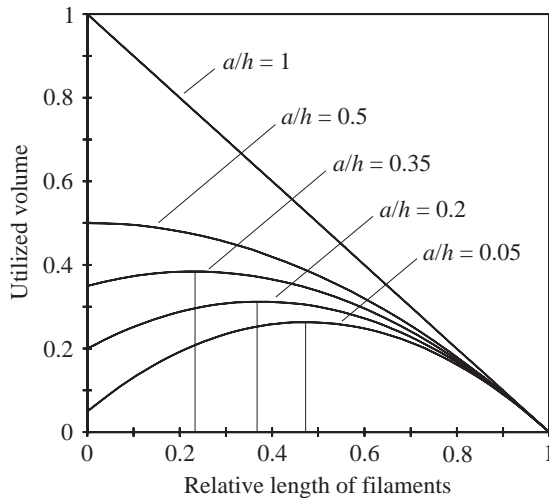


Fig. 5. The relationship between head capsule volume that can be used by muscle fibres ('utilized volume'; y axis) and the relative length of filaments f (x axis) for areas differing in the ratio of apodeme to head capsule surface area (a/h). The relationships were calculated using the equation: $\eta = (a/h - 1)f^2 + (1 - 2a/h)f + a/h$ (for derivation, see model 2 in the Appendix). Directly attached fibres ($f=0$) can use 100% of the head volume if $a/h=1$. For $a/h < 0.5$, filament-attached fibres ($f > 0$) make better use of the available head capsule volume and can therefore generate more force. Vertical lines indicate the maxima of the three lower curves. See text for further details.

little apodeme surface area would be available for the muscle fibres to attach directly. Filament-attached muscle fibres make better use of the available head capsule volume in these regions (Fig. 3D,E).

The distribution of filament-attached and directly attached muscle fibres with respect to the ratio of apodeme to head capsule surface area (a/h) is depicted by the curves in Fig. 5. The equation underlying these curves is derived from calculations describing the geometrical situations shown in Fig. 3D,E (see model 2, Appendix). For directly attached muscle fibres (relative length of filaments $f=0$), the proportion of the head volume utilized may reach 100% if the a/h is 1. For $a/h < 0.5$, filament attachment becomes necessary in order to maximize the utilized volume (in Fig. 5, the maxima of the curves depicting a/h values of 0.35, 0.2 and 0.05, respectively, occur at increasing filament lengths). This is the case in peripheral head regions where there is not enough apodeme surface area available for muscle fibres to attach directly (Figs 1C, 3B,D). The smaller the a/h ratio, the longer the filaments have to be to fill the space most efficiently with muscle fibres. This is the reason why the filaments vary in length within and among species and why, in some cases, they are not present at all (Fig. 1D-F). More efficient use of head volume means a larger overall power output or that the required muscular power can be generated within a smaller head capsule. An efficiently designed (hence smaller) head means that less energy has to be spent to move the body mass around, and a smaller head may also be more easy to manoeuvre.

Filaments need a much smaller apodeme surface area to attach to than do directly attached muscle fibres. Filament-attached fibres can thus make better use of the available head capsule surface area, resulting in a higher absolute number of muscle fibres (compare Fig. 3B and D with Fig. 3C and E, respectively). Moreover, filament-attached fibres may insert at an optimal angle at the apodeme because there is no additional 'cost' in terms of apodeme surface area as is the case in directly attaching fibres (see above). Fig. 3B shows that, in posterior head regions, filament-attached fibres may insert at very small angles with respect to the overall direction of pull, which results in a larger force vector in the required direction. Accordingly, their individual contribution to the resulting overall force is significantly larger than that of directly attached fibres for which the optimum angle is 45° (see above). The difference in overall power output due to the smaller attachment angle and the higher absolute number of muscle fibres acting in parallel (Fig. 3B,C) may be surprisingly large. The filament-attached fibres in the schematic example of Fig. 3B (20 fibres, mean angle of attachment 24.5°) would generate more than twice as much force as the directly attached fibres in Fig. 3C (12 fibres, angle of attachment 45°). Of course, on average, the filament-attached fibres are shorter, so that fewer sarcomeres shorten in series and the resulting movement generated by the arrangement depicted in Fig. 3B would not be as fast as that for the arrangement depicted in Fig. 3C.

Species-specific differences: filaments or direct fibre attachment?

It seems that the conditions can be defined relatively clearly under which filament-attached or directly attached fibres are advantageous. One might thus expect an optimal ratio of the two fibre types to be expressed in all ant species. Why, then, do we find among different species divergent designs and varying proportions of the fibre types ranging from virtual absence to almost sole presence of filament-attached fibres (Table 1)? Three tendencies emerge from our study which may account for this diversity.

First, the ratio of directly attached and filament-attached fibres depends on the behaviour and living conditions of a given species, just as is the case for the proportions of fast and slow muscle fibres (Gronenberg et al., 1997). Species that perform fast mandible movements rely on fast muscles composed of long muscle fibres which attach directly at small angles at the apodeme. Hence, fast movements generally require long head capsules to accommodate the long muscle fibres (e.g. the predatory *Harpegnathos saltator*; Fig. 2). In contrast, species depending on particularly forceful mandible movements, such as seed-cracking harvesting ants or leaf-cutting ants, generally have broad heads (compare *Atta sexdens* and *Harpegnathos saltator* in Fig. 2). In a broad head, more muscle fibres can be accommodated in parallel. However, broad heads feature relatively shorter apodemes, and hence a smaller apodeme surface area for the muscle fibres to attach to. For this reason,

more muscle fibres are filament-attached in these species. Moreover, in posterior head regions, filament-attached fibres have a force advantage over directly attaching fibres (see above). As a result, species requiring forceful mandible movements tend to have broad heads and many filament-attached fibres, whereas fast predators tend to feature longer heads and a greater proportion of directly attached muscle fibres in addition to a higher percentage of physiologically fast muscle fibres (Gronenberg et al., 1997). The relatively broad head of the ant *Myrmecia* sp. (Fig. 2) indicates that these ants can generate large forces with their long and sturdy mandibles. However, ants of the genus *Myrmecia* are also known for their fast-snapping mandibles (Gray, 1971b). This seeming exception from the tendency of ants performing fast mandible movements to feature long heads can be explained by several facts: (1) ants of the genus *Myrmecia* have particularly large brains, which probably require broad heads; (2) for unknown reasons, in the genera *Myrmecia*, *Amblyopone* and *Mystrium*, the mandible bases are set widely apart and thus require broad heads; and (3) *Myrmecia* sp. have very large heads and mandible closer muscles in absolute terms. Because head volume increases faster with increasing head size than does surface area, these ants need relatively larger attachment surfaces and hence broader heads and branched apodemes (Fig. 2). Nevertheless, *Myrmecia* sp. appear less specialized for speed of action than do *Harpegnathos saltator* (Fig. 2), even though they do perform fast mandible movements.

Second, there is a general tendency for smaller species (*Leptothorax sordidulus*, *Technomyrmex* sp. and *Gnamptogenys* sp.) and smaller individuals (*Camponotus rufipes* small workers versus soldiers) to feature more filament-attached fibres (Table 1; Paul et al., 1996). We do not understand the reasons for this tendency or its significance at present.

Third, the ranking of species according to their type of muscle fibre attachment (Table 1) to some extent reflects their phylogenetic relationships. The myrmeciine genus *Myrmecia* and the ponerine genera *Odontomachus*, *Diacamma*, *Harpegnathos* and *Ectatomma* all have substantially fewer filament-attached fibres and shorter filaments than the myrmicine or formicine genera studied (*Pogonomyrmex*, *Acanthognathos*, *Atta*, *Camponotus*), suggesting an evolutionary trend towards more and longer filaments. However, the former genera are predators relying mainly on rapid mandible action, while the latter are herbivorous or omnivorous and are probably less dependent on the speed of mandible movements. The apparent phylogenetic trend may thus only reflect different requirements in terms of mandible velocity.

To summarize, we conclude that muscle fibre attachment type in different species of ants depends both on body size and on phylogeny. However, the most significant determinants of the requirements for fast or forceful mandible movements in ant species are life-style variables such as feeding habit.

Appendix

Model 1: optimal angle of attachment to maximize power output

In principle, any real apodeme (left side of Fig. 4A) can be considered as being composed of two perpendicular surfaces, an x (horizontal) and a y (longitudinal) component (right side of Fig. 4A). In real apodemes, the x component is small (representing the apodeme base surfaces) and the y component is large (representing the long apodeme branches). Each directly attached fibre covers a portion of the apodeme surface. This portion (y_i , x_i in Fig. 4B) depends on the angle of attachment α and (except in the single case of $\alpha=45^\circ$) is different for the x and the y components of the apodeme (Fig. 4B):

$$y_i = d/\sin\alpha, \quad (1)$$

$$x_i = d/\cos\alpha, \quad (2)$$

where x_i , y_i are the attachment surfaces of a given fibre in the x or y directions, respectively, d is fibre diameter and α is the angle of attachment.

The total number i of fibres that can attach to a given apodeme is calculated as the quotient of the apodeme surface (x and y components) and the attachment surface of a single muscle fibre. Since fibres can attach to both sides of the longitudinal apodeme branches, the y component is doubled:

$$i = (2y/y_i) + (x/x_i), \quad (3)$$

where i is the maximum number of muscle fibres and x , y are the apodeme width and length, respectively.

The resultant force in the y direction (the principal direction of pull) of a single muscle fibre, $\mathbf{F}_i(\alpha)$, depends on the attachment angle:

$$\mathbf{F}_i(\alpha) = \mathbf{f}_i \cos\alpha, \quad (4)$$

where \mathbf{f}_i is the force produced by a single fibre (see Fig. 4B).

The individual fibres act concurrently to generate the total resultant force of the muscle, $\mathbf{F}(\alpha)$, which is equal to the sum of the force produced by all fibres:

$$\mathbf{F}(\alpha) = i\mathbf{F}_i(\alpha). \quad (5)$$

The optimal angle of attack between the apodeme and the muscle fibre should be 0° (equation 4; $\cos 0^\circ=1$); however, the attachment surface for a given fibre increases with decreasing attachment angle (equation 1) and would become infinitely large at 0° . At 90° , the attachment surface is at a minimum, which would allow the maximum number of fibres to be attached to a given apodeme. However, in this case, the resulting force would be zero (equation 4; $\cos 90^\circ=0$). Thus, the optimal mean angle of attachment for all fibres of a muscle will lie somewhere between 0° and 90° .

The total force $\mathbf{F}(\alpha)$ acting on the apodeme depends on fibre diameter, apodeme size and angles of attachment and can be calculated by combining equations 3 and 5:

$$\mathbf{F}(\alpha) = (\mathbf{f}_i/d)(\cos\alpha)[2y(\sin\alpha) + x(\cos\alpha)]. \quad (6)$$

Model 2: efficient use of head capsule volume and the mode of fibre attachment

This model is applicable to any region of the head capsule which reflects the geometrical relationships shown in Fig. 3D,E. The 'utilized' volume η is defined as the quotient of the volume V that actually contains muscle fibres and the overall volume V_{\max} that could be filled with fibres:

$$\eta = V/V_{\max}. \quad (7)$$

For simplicity, we treat V and V_{\max} as areas rather than volumes. Thus, the volume V_{\max} corresponds to the area of the parallelogram in Fig. 6, which is defined by its base h and its height l_{\max} :

$$V_{\max} = hl_{\max}, \quad (8)$$

where h is head capsule surface and l_{\max} is the distance between apodeme branch and head capsule.

The volume V occupied by the muscle fibres is:

$$V = a_v l, \quad (9)$$

where a_v is the virtual apodeme attachment surface and l is the perpendicular component of the fibre length (Fig. 6).

The virtual apodeme attachment surface a_v depends on the perpendicular component of the absolute filament length f_a and the apodeme attachment surface a :

$$a_v = m f_a + a, \quad (10)$$

where m is a linearity factor calculated from:

$$m = (h - a)/l_{\max}. \quad (11)$$

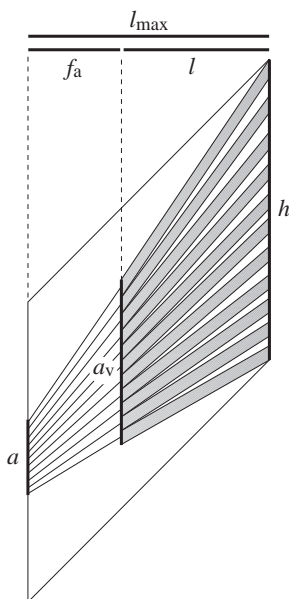


Fig. 6. Diagram illustrating the variables used to describe the use of head capsule volume by muscle fibres and to derive equation 13 (for details, see the Appendix, model 2). a , apodeme attachment surface; a_v , virtual apodeme attachment surface; f_a , perpendicular component of absolute filament length; h , head capsule surface; l , perpendicular component of fibre length; l_{\max} , perpendicular component of maximal fibre length.

Combining equations 11, 10 and 9 with equation 7 and substituting l for $(l_{\max} - f_a)$, equation 7 becomes:

$$\eta = (l_{\max} - f_a) \{ [(h - a)/l_{\max}] f_a + a \} / (h l_{\max}). \quad (12)$$

Defining the relative length of filaments f as $f = f_a/l_{\max}$ and simplifying equation 12 yields:

$$\eta = (a/h - 1) f^2 + (1 - 2a/h) f + a/h. \quad (13)$$

The curves plotted in Fig. 5 are calculated using equation 13 for different a/h ratios.

We thank Bert Hölldobler for providing ants and helpful suggestions, Karin Möller for help with histology, and Fritz Lehmann and Bert Hölldobler for comments on the manuscript. This work was supported by Deutsche Forschungsgemeinschaft (Gr 933/2 and Graduiertenkolleg 'Arthropodenverhalten').

References

- Alexander, R. McN.** (1983). *Animal Mechanics*. pp. 10–12. Oxford, London: Blackwell Scientific Publications.
- Alexander, R. McN.** (1988). *Elastic Mechanisms in Animal Movement*. p. 17. Cambridge: Cambridge University Press.
- Ali, T. M. M., Urbani, C. B. and Billen, J.** (1992). Multiple jumping behaviors in the ant *Harpegnathos saltator*. *Naturwissenschaften* **79**, 374–376.
- Baroni Urbani, C., Boyan, G. S., Billen, B., Billen, J. and Ali, T. M. M.** (1994). A novel mechanism of jumping in the Indian ant *Harpegnathos saltator* (Jerdon) (Formicidae, Ponerinae). *Experientia* **50**, 63–71.
- Baskin, R. J. and Paolini, P. J.** (1966). Muscle volume changes. *J. Gen. Physiol.* **49**, 387–404.
- Dietz, B. H. and Brandão, C. R. F.** (1993). Comportamento de caça e dieta de *Acanthognathis rudis* Brown and Kempf, com comentários sobre a evolução da predação em dacetini (Hymenoptera, Formicidae, Myrmicinae). *Rev. Bras. Ent.* **37**, 683–692.
- Gray, B.** (1971a). Notes on the biology of the ant species *Myrmecia dispar* (Clark) (Hymenoptera: Formicidae). *Insectes Sociaux* **18**, 71–80.
- Gray, B.** (1971b). Notes on the field behavior of two ant species *Myrmecia desertorum* Wheeler and *Myrmecia dispar* (Clark) (Hymenoptera: Formicidae). *Insectes Sociaux* **18**, 81–94.
- Gronenberg, W.** (1995). The fast mandible strike in the trap-jaw ant *Odontomachus*. I. Temporal properties and morphological characteristics. *J. Comp. Physiol. A* **176**, 391–398.
- Gronenberg, W., Brandao, C. R. F., Dietz, B. H. and Just, S.** (1998a). Trap-jaws revisited: the mandible mechanism of the ant *Acanthognathus*. *Physiol. Ent.* **23**, 227–240.
- Gronenberg, W. and Ehmer, B.** (1995). Tubular muscle fibers in ants and other insects. *Zoology* **99**, 68–80.
- Gronenberg, W., Hölldobler, B. and Alpert, G. D.** (1998b). Jaws that snap: the mandible mechanism of the ant *Mystrium*. *J. Insect Physiol.* **44**, 241–253.
- Gronenberg, W., Paul, J., Just, S. and Hölldobler, B.** (1997). Mandible muscle fibers in ants: Fast or powerful. *Cell Tissue Res.* **289**, 347–361.
- Gullan, P. J. and Cranston, P. S.** (1994). *The Insects: An Outline of*

- Entomology*. London, Glasgow, Weinheim, New York, Tokyo, Melbourne, Madras: Chapman & Hall.
- Hölldobler, B. and Wilson, E. O.** (1990). *The Ants*. Cambridge, MA: Belknap Press of Harvard University Press.
- Huxley, A. F.** (1974). Review lecture: Muscular contraction. *J. Physiol., Lond.* **243**, 1–43.
- Huxley, H. E.** (1965). The mechanism of muscular contraction. *Scient. Am.* **213**, 18–27.
- Jahromi, S. S. and Atwood, H. L.** (1969). Correlation of structure, speed of contraction and total tension in fast and slow abdominal muscles fibres of the lobster (*Homarus americanus*). *J. Exp. Zool.* **171**, 25–38.
- Janet, C.** (1905). *Anatomie de la Tete du Lasius niger*. Paris: Limoges.
- Janet, C.** (1907a). *Anatomie du Corselet et Histolyse des Muscles Vibrateurs, apres le Vol Nuptial, chez la Reine de la Fourmi* (*Lasius niger*). Paris: Limoges.
- Janet, C.** (1907b). Histolyse des muscles de mise en place des ailes, apres le vol nuptial, chez les reines de fourmis. *C.R. Acad. Sci. Paris* **1907**, 1–4.
- Just, S. and Gronenberg, W.** (1999). The control of mandible movements in the ant *Odontomachus*. *J. Insect Physiol.* (in press).
- Lang, F., Costello, W. J. and Govind, C. K.** (1977). Development of the dimorphic closer muscles of the lobster *Homarus americanus*. I. Regional distribution of muscle fibre types in adults. *Biol. Bull.* **152**, 75–83.
- Neville, A. C.** (1975). *Biology of the Arthropod Cuticle*. pp. 37–45, pp 355–368. Berlin: Springer.
- Paul, J., Just, S. and Gronenberg, W.** (1996). Functional morphology of tubular fibers in ant mandibular muscles: A comparative approach. *Proceedings of the 24th Göttingen Neurobiology Conference*. Vol. II. p. 100. Stuttgart, New York: Thieme.
- Pringle, J. W. S.** (1972). Arthropod muscle. In *The Structure and Function of Muscle* (ed. G. H. Bourne), pp. 491–541. New York, London: Academic Press.
- Snodgrass, R. E.** (1935). *Principles of Insect Morphology*. pp. 48–69. New York: McGraw-Hill Book Company, Cornell University Press (reprint 1993).
- Tautz, J., Hölldobler, B. and Danker, T.** (1994). The ants that jump: Different techniques to take off. *Zoology* **98**, 1–6.
- Tregear, R. T. and Marston, S. B.** (1979). The crossbridge theory. *Annu. Rev. Physiol.* **41**, 723–736.
- Wilson, E. O.** (1985). The sociogenesis of insect colonies. *Science* **228**, 1489–1495.